Published in final edited form as:
Can J Physiol Pharmacol. 2011 October ; 89(10): 723–736. doi:10.1139/y11-070.

Multiple arrhythmic syndromes in a newborn, owing to a novel mutation in *SCN5A*

Kirstine Calloe,
Danish National Research Foundation Centre for Cardiac Arrhythmia, Department of Biomedical Sciences, University of Copenhagen, Blegdamsvej 3, DK-2200 Copenhagen N, Denmark

Nicole Schmitt,
Danish National Research Foundation Centre for Cardiac Arrhythmia, Department of Biomedical Sciences, University of Copenhagen, Blegdamsvej 3, DK-2200 Copenhagen N, Denmark

Soren Grubb,
Danish National Research Foundation Centre for Cardiac Arrhythmia, Department of Biomedical Sciences, University of Copenhagen, Blegdamsvej 3, DK-2200 Copenhagen N, Denmark

Ryan Pfeiffer,
Department of Experimental Cardiology, Masonic Medical Research Laboratory, 2150 Bleecker Street, Utica, NY 13501, USA; Masonic Medical Research Laboratory, Utica, NY 13413 USA

Jens-Peter David,
Danish National Research Foundation Centre for Cardiac Arrhythmia, Department of Biomedical Sciences, University of Copenhagen, Blegdamsvej 3, DK-2200 Copenhagen N, Denmark; Masonic Medical Research Laboratory, Utica, NY 13413 USA

Ronald Kanter,
Duke University Medical Center, Durham, NC 27710, USA; Masonic Medical Research Laboratory, Utica, NY 13413 USA

Jonathan M. Cordeiro, and
Department of Experimental Cardiology, Masonic Medical Research Laboratory, 2150 Bleecker Street, Utica, NY 13501, USA; Masonic Medical Research Laboratory, Utica, NY 13413 USA

Charles Antzelevitch
Department of Experimental Cardiology, Masonic Medical Research Laboratory, 2150 Bleecker Street, Utica, NY 13501, USA; Masonic Medical Research Laboratory, Utica, NY 13413 USA

Abstract

Background—Mutations in the *SCN5A* gene have been linked to Brugada syndrome (BrS), conduction disease, Long QT syndrome (LQT3), atrial fibrillation (AF), and to pre- and neonatal ventricular arrhythmias.

Objective—The objective of this study is to characterize a novel mutation in $Na_v1.5$ found in a newborn with fetal chaotic atrial tachycardia, postpartum intraventricular conduction delay, and QT interval prolongation.

Methods—Genomic DNA was isolated and all exons and intron borders of 15 ion-channel genes were sequenced, revealing a novel missense mutation (Q270K) in *SCN5A*. $Na_v1.5$ wild type (WT) and Q270K were expressed in CHO-K1 with and without the $Na_v\beta1$ subunit.

Corresponding author: Kirstine Calloe (kirstinec@sund.ku.dk)..

Results—Patch-clamp analysis showed ~40% reduction in peak sodium channel current (I_{Na}) density for Q270K compared with WT. Fast and slow decay of I_{Na} were significantly slower in Q270K. Steady-state activation and inactivation of Q270K channels were shifted to positive potentials, and window current was increased. The tetrodotoxin-sensitive late I_{Na} was increased almost 3-fold compared with WT channels. Ranolazine reduced late I_{Na} in WT and Q270K channels, while exerting minimal effects on peak I_{Na}.

Conclusion—The Q270K mutation in *SCN5A* reduces peak I_{Na} while augmenting late I_{Na}, and may thus underlie the development of atrial tachycardia, intraventricular conduction delay, and QT interval prolongation in an infant.

Keywords

arrhythmia; LQT syndrome; Brugada syndrome; atrial fibrillation; electrophysiology; genetics; $Na_v1.5$; neonate

Introduction

The cardiac sodium current (I_{Na}) is responsible for the rapid depolarization of cardiomyocytes as well as for the propagation of the action potential throughout the heart. The current inactivates rapidly, although a small fraction of channels may reopen during the plateau phase of the cardiac action potential, resulting in a persistent or late inward current (I_{NaL}) (Maltsev et al. 1998). I_{NaL} is important in determining the duration of the cardiac action potential (Attwell et al. 1979).

I_{Na} is carried by the pore forming α-subunit, $Na_v1.5$, and the biophysical properties of $Na_v1.5$ are regulated by multiple proteins, such as the β-subunits ($Na_vβ1–4$) and anchoring proteins, all of which form a macromolecular complex. Some of these proteins also regulate targeting and trafficking of the macromolecular complex to the cell membrane (reviews by Meadows and Isom 2005; Abriel 2010). Several arrhythmia syndromes have been linked to mutations in genes encoding $Na_v1.5$ or in the ancillary subunits that contribute to I_{Na}. Brugada syndrome (BrS), conduction disease, and sick sinus syndrome have been linked to a reduction in I_{Na} (review by Zimmer and Surber 2008). Mutations resulting in a gain of function have been linked to Long QT Syndrome Type 3 (LQT3), as well as to prenatal and ventricular arrhythmias in newborns (Wang et al. 2008) and sudden infant death syndrome (SIDS) (Ackerman et al. 2001; Wedekind et al. 2001; Schwartz et al. 2002; Valdivia et al. 2002; Arnestad et al. 2007; Wang et al. 2007).

These syndromes may overlap in the same patient or among different members of a family carrying the same mutation (Bezzina et al. 1999; Veldkamp et al. 2000; Kyndt et al. 2001; Grant et al. 2002; Remme et al. 2008). Variations in phenotype expression are thought to be attributable to the severity of the disease-causing mutation as well as the possible co-existence of other genetic variations, including single nucleotide polymorphisms (SNP), which are not disease-causing, but which can affect arrhythmia susceptibility. For example, the SNP K897T in the $K_V11.1$ channel has been demonstrated to increase arrhythmia susceptibility in carriers of $K_V11.1$ mutations with low penetrance (Crotti et al. 2005; Nof et al. 2010).

Here, we describe a newborn with severe atrial tachycardia, conduction abnormalities, and QT interval prolongation. Genetic analysis revealed a substitution of a glutamine (Q) to a lysine (K) at position 270 (Q270K) in the 5th transmembrane segment (S5) of domain 1 (D1) of the $Na_v1.5$ sodium channel. The Q270K mutation resulted in a reduction in peak I_{Na} but a gain of function in late I_{Na}, compared with wild-type (WT), and thus is suspected to

generate the substrate for both the slowed conduction and the LQT3 phenotypes observed in this patient.

Materials and methods

Genetic analysis

Genomic DNA was prepared from peripheral blood lymphocytes of the patient and available family members. All known exons of SCN5A, SCN1B, SCN3B, KCNH2, KCNQ1, KCNJ2, KCNE1, KCNE2, KCNE3, KCND3, KCNIP2, KCNJ11, CACNA1C, CACNB2b, and *CACNA2D1* were amplified with intronic primers and sequenced in both directions. No mutations were detected except in *SCN5A*. The mutation was absent in 200 unrelated control individuals with the same ethnic background. All clinical and genetic studies conformed to the principles outlined in the *Declaration of Helsinski* and written informed consent was obtained according to protocols approved by the local Institutional Review boards.

Cloning

Mutagenesis was performed on a plasmid containing cDNA for $hNa_v1.5$ that refers to isoform 2 (NM_000335) and is known as hH1c (i.e., it lacks Q1077). Of note, nomenclature of patient mutations refers to isoform 1. The point mutation Q270K (CAG → AAG) in $hNa_v1.5$ was introduced using mutated oligonucleotide extension (PfuTurbo Polymerase, Stratagene, La Jolla, California, USA) from a plasmid template (hNav1.5 in pcDNA3.1), digested with DpnI (Fermentas, St. Leon-Roth, Germany) and transformed into *E. coli* XL1 Blue cells. $Na_v\beta1$ in pcDNA3.1 was obtained by subcloning from pIRES-hβ1-CD8: a kind gift of H. Abriel (University of Bern, Switzerland). All constructs were verified by DNA sequencing of the cDNA insert (Macrogen, Inc., Seoul, Korea).

Electrophysiology

Chinese hamster ovary (CHO-K1) cells were transfected with 2 μg $hNa_v1.5$, $hNa_v1.5$_Q270K, or $hNa_v1.5$ + $hNa_v1.5$_Q270K in a 1:1 molar ratio. For co-expression of $hNa_v1.5$ or $hNa_v1.5$_Q270K with $hNa_v\beta1$, 1 μg $Na_v1.5$ (WT or Q270K) was mixed with 1 μg $hNa_v\beta1$; eGFP (0.2 μg) was included to identify transfected cells. Transfections were performed using Lipofectamine and Plus reagent (GIBCO, Invitrogen, Carlsbad, Calif.) according to the manufacturer's instruction. Cells were kept in Dulbecco's modified Eagle's medium (University of Copenhagen, Denmark) supplemented with 10% fetal calf serum (GIBCO) and 40 mg/L L-proline at 37 °C in 5% CO_2. Currents were recorded 2–3 days post-transfection using a MultiClamp 700B amplifier and MultiClamp Commander (Molecular Devices, Axon Instruments, Sunnyvale, Calif.). Cells were superfused with a solution containing (in mmol/L): 130 NaCl, 5 KCl, 1.8 $CaCl_2$, 1.0 $MgCl_2$, 2.8 Na acetate, 10 HEPES, 10 glucose, pH adjusted to 7.3 with NaOH. Patch pipettes were fabricated from borosilicate glass capillaries (Module Ohm, Herlev, Denmark) and had resistances between 1.5–2 MΩ when filled with pipette solution (mmol/L): 10 KCl, 105 CsF, 10 NaCl, 10 HEPES, 10 EGTA, and 5 TEA–Cl, pH adjusted to 7.2 with CsOH. Electronic compensation of series resistance to 70%–85% was applied to minimize voltage errors. All analog signals were acquired at 10–50 kHz, filtered at 6 kHz, digitized with a Digidata 1440 converter (Axon Instruments), and stored using pClamp10 software (Axon Instruments). All recordings were made at room temperature (20–22 °C). Data were analysed using pClamp10 software (Axon Instruments) and Prism 4.03 (GraphPad Software, Inc., La Jolla, Calif.). Mean ± SEM values are shown, statistical significance (*, $p < 0.05$) was evaluated as appropriate by one-way ANOVA followed by Student–Newman–Keuls post test, or by paired or unpaired Student's *t* test.

Drugs

Tetrodotoxin (TTX, 10 μmol/L) was added from a 100 mmol/L stock of TTX-citrate (Tocris Bioscience, Bristol, UK) dissolved in water that was double-distilled using the Milli-Q system (Millipore Corp., Bedford, Massachusetts, USA). Ranolazine (Gilead, Palo Alto, Calif.) was made as a stock solution of 10 mmol/L DMSO, and used at a final concentration of 50 μmol/L.

Results

Case presentation

Owing to polyhydramnios and fetal tachycardia, the female patient was prematurely born at week 34 by Cesarian section. Her birth weight was 2.04 kg. Fetal tachycardia was first diagnosed at 29 weeks gestation, and best characterized by fetal echocardiography as nonsustained but incessant chaotic atrial tachycardia or atrial fibrillation, with atrial rates as rapid as 500–600 beats per minute (bpm) and variable ventricular response (Fig. 1A). The irregularity of the atrial rhythm was not consistent with fetal atrial flutter. Runs were interrupted by brief periods of sinus rhythm at 140 bpm. The rhythm was controlled with maternal enteral sotalol (120 mg twice daily). Subsequent fetal echocardiograms demonstrated mostly sinus rhythm (Fig. 1B), with short bursts of regular atrial tachycardia at rates of up to 480 bpm with variable atrioventricular (AV) conduction. The patient's mother was asymptomatic, and her first pregnancy was carried to full term without any problems.

The patient's initial rhythm within moments of delivery was atrial flutter, which degenerated into ventricular fibrillation (Figs. 2A and 2B). During atrial flutter, the ventricular rate was within the normal range (144 bpm) owing to 3:1 AV block. Thirty minutes post-natally, and following defibrillation and a single intravenous dose of amiodarone (5 mg/kg), the patient became asystolic. Successful resuscitation included transesophageal atrial pacing, owing to persistent bradycardia. There was intraventricular conduction delay with QRS duration as long as 119 ms during both atrial pacing and normal sinus rhythm, up to 7 days post-natally, and well beyond plausible effects of transplacental sotalol and the single small intravenous dose of amiodarone (Fig. 2C). This observation was in the presence of β-adrenergic agents, during normal electrolyte and acid-base status and after marked improvement in ventricular function by echocardiography. Echocardiography also revealed a bicuspid aortic valve. The patient's initial course was further complicated by pulmonary hemorrhage and the need for oscillatory assisted ventilation, also by bifrontal subdural, interventricular, and periventricular hemorrhages, as well as hemodynamic instability, requiring multiple vasopressor agents (intra venous dopamine, epinephrine, and vasopressin).

Despite the placement of temporary epicardial atrial pacing wires by limited sternotomy and attempts at overdrive atrial pacing, recurrent episodes of hemodynamically unstable atrial tachycardia required DC cardioversion while the patient was 1–7 days old. Intravenous amiodarone was loaded while the patient was 7–10 days old, for a total of 30 mg/kg, but resulted in marked QTc prolongation (Fig. 2D). Despite normal acid-base status and serum electrolytes, torsade de pointes (TdP) following long-short ventricular sequences (Fig. 2E) occurred on 4 occasions when the patient was 10-12 days old, requiring discontinuation of amiodarone. Quinidine-sulfate (10 mg/kg every 6 h) was administered enterally. Following the first dose of quinidine, she had no further atrial or ventricular arrhythmias. To limit future pause-dependent TdP, a permanent dual-chamber pacemaker was implanted on day 17, and she was discharged from the hospital when she was 37 days old. At 23 months of age, the patient had experienced no episodes of syncope, seizures, or other signs of paroxysmal tachycardias. Her parents had discontinued quinidine at approximately 6 months of age. Twelve lead electrocardiogram in the drug-free state showed QT interval

prolongation with a QTc interval of 466 ms (Fig. 2F), but normalization of the intraventricular conduction delay. In summary, this infant displayed 3 clinical electrophysiologic abnormalities, which were thought to be independent of antiarrhythmic drug effects and metabolic disturbances: fetal irregular atrial tachycardia or atrial fibrillation, post-natal intraventricular conduction delay, and QT interval prolongation

Analysis of the patient's DNA showed a heterozygous C to A transition at nucleotide position 808 in exon 7 in *SCN5A* (Fig. 3A). This transition predicted a substitution of a highly conserved glutamine (Q) to a lysine (K) at position 270 (Q270K) in S5 of domain I of $Na_v1.5$ (Fig. 3B).

Electrophysiological characterization of Nav1.5_Q270K

WT $Na_v1.5$, Q270K or WT/Q270K (1:1 ratio to mimic the heterozygote state) were expressed in CHO-K1 cells. Both WT and Q270K channels exhibited a fast activating and inactivating current (Fig. 4A). However, Q270K had a reduced peak current density (Fig. 4B) and double exponential fits to the current decay showed that both τ_{slow} and τ_{fast} were significantly slower for Q270K (Fig. 4C). The relative weights of the pre-exponential factors for τ_{fast}/τ_{total} were calculated (Fig. 4D), showing that the relative contribution of the fast component was reduced for Q270K. For WT/Q270K an intermediate phenotype was found.

Steady-state activation curves were calculated by normalizing the currents shown in Fig. 5 to (V_m–E_K). The $V_{1/2}$ of steady-state activation was significantly shifted to more depolarized values for Q270K compared with WT, with $V_{1/2} = -34.4 \pm 0.2$ mV ($n = 8$) for WT, and $V_{1/2} = -28.6 \pm 0.3$ mV ($n = 7$) ($p < 0.0001$) for Q270K (Fig. 5A). Steady-state inactivation was addressed by a prepulse-pulse protocol (Fig. 5A). For WT, the $V_{1/2}$ of inactivation was -71.2 ± 0.3 mV ($n = 9$) and for Q270K significantly shifted to $V_{1/2} = -61.3 \pm 0.8$ mV ($n = 6$, $p < 0.0001$). The shift in $V_{1/2}$ for activation and inactivation resulted in larger window currents (magnified part of Fig. 5A). Within this window of voltages, a small percentage of channels are not inactivated and are thus available for activation.

Recovery from inactivation of WT and Q270K was addressed by a 2-pulse protocol (Fig. 5B). At −120 mV and −100 mV, the recovery of Q270K and WT was similar, however at −80 mV, Q270K recovered significantly faster from inactivation than for WT, with $\tau = 5.8 \pm 0.22$ ms for WT ($n = 8$) and 4.8 ± 0.21 ms for Q270K ($n = 6$, $p = 0.0077$).

The interaction between $Na_v1.5$ and the $Na_v\beta1$ has been reported to include the extracellular domain of $Na_v\beta1$ and the extracellular loop between S5 and S6 in D1 and D4 of $Na_v1.5$ (Makita et al. 1996; McCormick et al. 1999). As the Q270K mutation resides in D1-S5 of $Na_v1.5$, suggesting that the Q270k mutation could interfere with interaction between $Na_v1.5$ and $Na_v\beta1$, we repeated the functional studies in the presence of the $Na_v\beta1$ subunit. $Na_v1.5$ WT, Q270K, or WT/Q270K were co-expressed with $Na_v\beta1$ (1:1 ratio) in CHO-K1 cells. As $Na_v\beta1$ increased current density in agreement with previous reports (Qu et al. 1995; Fahmi et al. 2001; Bezzina et al. 2003; Herfst et al. 2003), only half the amount of $Na_v1.5$ DNA was used compared with the experiments without $Na_v\beta1$.

Similar to the results for experiments without $Na_v\beta1$, peak current density was reduced for Q270K/$Na_v\beta1$ compared with WT/$Na_v\beta1$ (Fig. 6A), and WT/Q270K/$Na_v\beta1$ had an intermediate phenotype (data not shown). The current decay (both τ_{slow} and τ_{fast}) was significantly slower for Q270K/$Na_v\beta1$ over a range of voltages (Fig. 6B), and for Q270K/$Na_v\beta1$ the relative weight of the fast component was lower (Fig. 6C).

Similar to the results in the absence of $Na_v\beta1$, a significant shift to more positive potentials was observed in $V_{1/2}$ for activation and inactivation for Q270K/$Na_v\beta1$ compared with WT/

$Na_v\beta1$. The $V_{1/2}$ of activation was −31.4 ± 0.4 mV for WT/$Na_v\beta1$ (n = 10) and −26.7 ± 0.4 mV for Q270K/$Na_v\beta1$ (n = 9, $p < 0.0001$). $V_{1/2}$ of inactivation was −77.7 ± 0.6 mV for WT/$Na_v\beta1$ (n = 9) and −61.2 ± 0.5 mV for Q270K/$Na_v\beta1$ (n = 8, $p < 0.0001$), (Fig. 6D), resulting in increased window currents. Time-dependent recovery from inactivation for WT/$Na_v\beta1$ and Q270K/$Na_v\beta1$ was investigated using holding potentials of −120 mV, −100 mV, and −80 mV. For all holding potentials, Q270K/$Na_v\beta1$ recovered significantly faster than WT/$Na_v\beta1$ (Fig. 6E).

Our results show that current decay was significantly slower for the Q270K mutation, and that window currents were increased. This prompted us to address the question as to whether Q270K has a larger persistent or late current than WT. WT/$Na_v\beta1$ and Q270K/$Na_v\beta1$ currents were activated by a 1 s step to −45 mV in the absence or presence of 10 μmol/L TTX for both Q270K and WT channels (Figs. 7A and 7B). Currents recorded in presence of TTX were digitally subtracted from controls, and the ratio between TTX sensitive peak and late currents were calculated, revealing a 3-fold increase in Q270K late current compared with WT (Fig. 7C).

As the Q270K mutation affected several gating processes of the $Na_v1.5$ channel, we measured I_{Na} using action potential voltage clamp techniques (Magyar et al. 2004). It is well established that I_{to} is absent in the neonatal ventricle in virtually all mammalian species (Jeck and Boyden 1992; Plotnikov et al. 2004; Shimoni et al. 1997) and it is likely that newborn humans also lack ventricular I_{to}. In the next next series of experiments, a previously recorded neonatal canine ventricular action potential waveform was used to activate WT/$Na_v\beta1$or Q270K/$Na_v\beta1$ current (Fig. 8A). Holding potentials of either −60 mV or −120 mV were used. At −60 mV, $Na_v1.5$ was fully inactivated (Fig. 8A) and the recorded current represents endogenous current. The recordings obtained at −6 0 mV were digitally subtracted from the recordings obtained at −120 mV (Fig. 8B). During the initial part of the action potential, the fast activating and inactivating I_{Na} transient dominated; however, during the plateau phase a persistent small I_{Na} current was present. Similar to the findings using TTX, the ratio of late current relative to peak current was 3-fold higher for Q270K compared with WT (Fig. 8C).

Ranolazine (50 μmol/L) has been shown to preferentially block late $Na_v1.5$ current, both for WT and for LQT3 mutants (Fredj et al. 2006). We next tested the effect of 50 μmol/L ranolazine on WT/$Na_v\beta1$ and Q270K/$Na_v\beta1$. Currents were activated by a −20 mV depolarization and recorded in the absence and presence of ranolazine (Figs. 9A-9B). Ranolazine had a minor but significant effect on both WT and Q270K peak currents (Fig. 9C). Similar to previous reports (Fredj et al. 2006), we found a relatively larger block of the late current for both WT and Q270K. The currents recorded in the presence of ranolazine were digitally subtracted from controls and the ranolazine-sensitive peak current, and late currents were calculated as well as the ratio between ranolazine sensitive peak and late current (Fig. 9C).

Discussion

In this study, we identified a Q270K substitution in $Na_v1.5$ in a neonate with severe cardiac arrhythmia, including fetal chaotic atrial tachycardia or fibrillation, intraventricular conduction delay, and prolonged QT intervals. Although the patient's early history was complicated by pulmonary hemorrhage, intracranial hemorrhage, hemodynamic instability, and treatment with vasopressor agents, the chaotic atrial tachycardia existed in utero prior to maternal antiarrhythmic drug application, and intraventricular conduction delay would not be an expected sequela of those noncardiac co-morbidities in an otherwise normal

electrolyte and acid–base state. At age 23 months, the QTc interval was 466 ms after antiarrhythmic drugs had been discontinued.

The 40% reduction of Q270K peak currents may explain the conduction delay. Discriminating intraventricular conduction delay from a true Brugada pattern may be less clear in infants compared with adults, as previously published electrocardiographic examples of BrS in children have not always conformed to strict diagnostic criteria (Priori et al. 2000; Beaufort-Krol et al. 2005). Despite equal genetic transmission of BrS, the clinical phenotype is 8–10 times more prevalent in males than in females, and BrS typically affects individuals in the 4th decade of life (Antzelevitch et al. 2005). Thus, the observation that the patient (a female newborn) exhibited a phenotype consistent with previously reported cases of childhood BrS is interesting. Experimental studies suggest that the presence of a prominent transient outward current (I_{to}) predisposes the myocardium to the development of the BrS by permitting the expression of a prominent phase 1 (Calloe et al. 2009). However, it is well established that I_{to} is virtually absent in the neonatal ventricle in all mammalian species studied (Jeck and Boyden 1992; Plotnikov et al. 2004; Trépanier-Boulay et al. 2004), and it is likely that newborn humans also lack I_{to}. This could account for the absence of a classic coved or saddleback ST segment pattern in this infant's right precordial leads. This does not explain why quinidine, which is known to be antiarrhythmic in the setting of BrS, likely due to inhibition of I_{to}, was effective in suppressing the arrhythmias in this patient.

The Q270K mutation is located proximal to the extracellular loop of $Na_v1.5$ that has been shown to be involved in interaction with $Na_v\beta1$ (Makita et al. 1996; McCormick et al. 1999), however, the effects of Q270K in absence or presence of $Na_v\beta1$ were qualitatively similar, suggesting that the mutation does not interfere with $Na_v1.5$ and $Na_v\beta1$ interaction.

Besides the reduction of Q270K peak current, inactivation was slower, and the $V_{1/2}$ of steady-state inactivation shifted resulted in larger window currents for the mutant. The slower decay of INa and increased window current could suggest that the Q270K mutation is interfering with fast inactivation of $Na_v1.5$. Fast inactivation of $Na_v1.5$ involves binding of a cluster of hydrophobic amino acids (the inactivation particle) positioned in the D3–D4 linker (West et al. 1992; Kellen-berger et al. 1997) to domains of S6 in D4 as well as the intracellular loops between D3 S4/S5 (Smith and Goldin 1997), D4 S4/S5 (McPhee et al. 1998), and D4 S6 (McPhee et al. 1995), and thereby closing the pore. Furthermore, inactivation is coupled to activation as movement of the voltage sensing S4 region of D4 generates the signal for inactivation (Chanda and Bezanilla 2002). Previously reported LQT3 mutations cluster in these regions (review by Zimmer and Surber 2008). However, mutations resulting in increased persistent current have been found outside these regions, such as the transmembrane regions (Wang et al. 2007), as well as the extracellular domain of D1 at S216L (Wang et al. 2007). The Q270K mutation resides in transmembrane segment S5 of D1, and how the Q270K destabilizes the inactivated state cannot be easily explained in terms of the current knowledge of sodium channel structure–function relationships, suggesting that other regions of the sodium channel are important for fast inactivation.

Our results demonstrated that current decay was significantly slowed by the Q270K mutation, and that the window current was increased, which prompted us to investigate whether late current was also affected. An increased late current was confirmed by experiments with TTX. Since impedance is high during the action potential plateau (Spitzer et al. 2006), the opening of even a few channels can greatly influence action potential duration. The Q270K mutation significantly increased the fraction of late current, with I_{NaL} = 0.16 ± 0.03% (n = 6) for WT and 0.54 ± 0.01% (n = 6, p = 0.032) for Q270K. These numbers are in agreement with previous results showing residual current to be 0.15% of the

peak current for WT $Na_v1.5$ channels (Dumaine et al. 1996). Also, in LQT3 mutant channels such as ΔKPQ, which cause a large increase in late currents, the fraction of late currents is still less than 5% (Dumaine et al. 1996).

Several reports have linked *SCN5A* mutations with increased I_{NaL}, and (or) increased window currents, to ventricular arrhythmias and SIDS (Ackerman et al. 2001; Lupoglazoff et al. 2001; Wedekind et al. 2001; Valdivia et al. 2002; Chang et al. 2004; Arnestad et al. 2007; Wang et al. 2008; Huang et al. 2009; Ruan et al. 2010). In a Norwegian study, 201 patients diagnosed with SIDS were screened for mutations in genes associated with LQTS. Mutations and rare variants were found in 26 cases: 4 patients harboured mutations in *SCNA5*, causing an increased I_{NaL}, and 4 had rare variants in *SCNA5*, also causing increased I_{NaL} (Arnestad et al. 2007), suggesting that increased I_{NaL} is an important genetic risk factor for SIDS. Although the proband initially had a normal baseline QTc of 421 ms, amiodarone treatment increased the QTc interval to 491 ms (Fig. 2D) and triggered several episodes of TdP (Fig. 2E). The torsadogenic effect of intravenous amiodarone during periods of normal electrolyte and acid–base status is very unusual in an infant, but could have been explained by the additional influence of intracranial hemorrhage. However, amiodarone-induced TdP has been associated with an increase in I_{NaL} in both experimental and clinical studies (Lehtonen et al. 2007; Remme and Bezzina 2007; Wegener et al. 2008; Wu et al. 2008) and the effect of amiodarone to induce TdP in our proband could be associated with the increased I_{NaL} induced by the Q270K mutation.

Gain of function, including positive shifts in steady-state inactivation of $Na_v1.5$, have also been linked to lone atrial fibrillation (Makiyama et al. 2008; Li et al. 2009) or atrial fibrillation in association with LQT3 (Benito et al. 2008). The increased I_{NaL} may cause early after-depolarizations and triggered activity (Benito et al. 2008; Makiyama et al. 2008), and thus may contribute to the development of atrial flutter in the patient.

The increase in persistent current (Fig. 7) prompted us to test the effect of ranolazine on the Q270K mutation. Ranolazine has previously been demonstrated to be a potent blocker of I_{NaL} induced by LQT3 mutations (Fredj et al. 2006; Bank-ston et al. 2007) and has been found to be effective in antagonizing the proarrhythmic effects of I_{NaL} in pharmacological models of LQT3 (Song et al. 2004; Wu et al. 2004). Ranolazine has also been shown to be effective in abbreviating QTc in patients with congenital LQT3 (Moss et al. 2008). We found that ranolazine preferentially blocked I_{NaL} for both WT and Q270K, however this preference was greater for the Q270K compared with WT, suggesting that ranolazine might be of benefit in this setting because of its actions to reduce the LQT3 phenotype without aggravating the conduction slowing produced by this mutation.

Conclusion

The Q270K mutation in $Na_v1.5$ reduces peak current density while augmenting late I_{Na}, and thus may underlie the development of neonatal life-threatening arrhythmias characterized by an overlap syndrome consisting of chaotic atrial tachycardia, intraventricular conduction delay, and QT interval prolongation.

Limitations

Although we used a constant molar ratio of multiple genes to ensure proper expression of both gene products, it is difficult to determine whether an individual cell actually expressed the 2 subunits in the same proportion. We assume that a cell incorporates both subunits based on our observations that when eGFP was co-transfected in a 1/10 ratio with the genes of interest, all cells expressing eGFP also expressed I_{Na}.

Acknowledgments

The Danish National Research Foundation; the National Institutes of Health (HL47678 to C.A.]; the Masons of New York State and Florida; and the Memorial Foundation of Eva and Henry Fraenkel.

References

Abriel H. Cardiac sodium channel Na(v)1.5 and interacting proteins: physiology and pathophysiology. J. Mol. Cell. Cardiol. 2010; 48(1):2–11. doi:10.1016/j.yjmcc.2009.08.025. PMID:19744495. [PubMed: 19744495]

Ackerman MJ, Siu BL, Sturner WQ, Tester DJ, Valdivia CR, Makielski JC, Towbin JA. Postmortem molecular analysis of SCN5A defects in sudden infant death syndrome. JAMA. 2001; 286(18): 2264–2269. doi:10.1001/jama.286.18.2264. PMID:11710892. [PubMed: 11710892]

Antzelevitch C, Brugada P, Borggrefe M, Brugada J, Brugada R, Corrado D, et al. Brugada syndrome: report of the second consensus conference. Endorsed by the Heart Rhythm Society and the European Heart Rhythm Association. Circulation. 2005; 111(5):659–670. doi:10.1161/01.CIR. 0000152479.54298.51. PMID:15655131. [PubMed: 15655131]

Arnestad M, Crotti L, Rognum TO, Insolia R, Pedrazzini M, Ferrandi C, et al. Prevalence of long-QT syndrome gene variants in sudden infant death syndrome. Circulation. 2007; 115(3):361–367. doi: 10.1161/CIRCULATIONAHA.106.658021. PMID: 17210839. [PubMed: 17210839]

Attwell D, Cohen I, Eisner D, Ohba M, Ojeda C. The steady state TTX-sensitive ("window") sodium current in cardiac Purkinje fibres. Pflugers Arch. 1979; 379(2):137–142. doi:10.1007/ BF00586939. PMID:571107. [PubMed: 571107]

Bankston JR, Yue M, Chung W, Spyres M, Pass RH, Silver E, et al. A novel and lethal de novo LQT-3 mutation in a newborn with distinct molecular pharmacology and therapeutic response. PLoS ONE. 2007; 2(12):e1258. doi:10.1371/journal.pone. 0001258. PMID:18060054. [PubMed: 18060054]

Beaufort-Krol GC, van den Berg MP, Wilde AA, Van Tintelen JP, Viersma JW, Bezzina CR, Bink-Boelkens MTE. Developmental aspects of long QT syndrome type 3 and Brugada syndrome on the basis of a single SCN5A mutation in childhood. J. Am. Coll. Cardiol. 2005; 46(2):331–337. doi: 10.1016/j. jacc.2005.03.066. PMID:16022964. [PubMed: 16022964]

Benito B, Brugada R, Perich RM, Lizotte E, Cinca J, Mont L, et al. A mutation in the sodium channel is responsible for the association of long QT syndrome and familial atrial fibrillation. Heart Rhythm. 2008; 5(10):1434–1440. doi:10.1016/j.hrthm.2008.07. 013. PMID:18929331. [PubMed: 18929331]

Bezzina C, Veldkamp MW, van den Berg MP, Postma AV, Rook MB, Viersma JW, et al. A single Na(+) channel mutation causing both long-QT and Brugada syndromes. Circ. Res. 1999; 85(12): 1206–1213. PMID:10590249. [PubMed: 10590249]

Bezzina CR, Rook MB, Groenewegen WA, Herfst LJ, van der Wal AC, Lam J, et al. Compound heterozygosity for mutations (W156X and R225W) in SCN5A associated with severe cardiac conduction disturbances and degenerative changes in the conduction system. Circ. Res. 2003; 92(2):159–168. doi:10.1161/01. RES.0000052672.97759.36. PMID:12574143. [PubMed: 12574143]

Calloe K, Cordeiro JM, Di Diego JM, Hansen RS, Grunnet M, Olesen SP, Antzelevitch C. A transient outward potassium current activator recapitulates the electrocardiographic manifestations of Brugada syndrome. Cardiovasc. Res. 2009; 81(4):686–694. doi:10.1093/cvr/cvn339. PMID: 19073629. [PubMed: 19073629]

Chanda B, Bezanilla F. Tracking voltage-dependent conformational changes in skeletal muscle sodium channel during activation. J. Gen. Physiol. 2002; 120(5):629–645. doi:10.1085/jgp. 20028679. PMID:12407076. [PubMed: 12407076]

Chang CC, Acharfi S, Wu MH, Chiang FT, Wang JK, Sung TC, Chahine M. A novel SCN5A mutation manifests as a malignant form of long QT syndrome with perinatal onset of tachycardia/ bradycardia. Cardiovasc. Res. 2004; 64(2):268–278. doi:10. 1016/j.cardiores.2004.07.007. PMID: 15485686. [PubMed: 15485686]

Crotti L, Lundquist AL, Insolia R, Pedrazzini M, Ferrandi C, De Ferrari GM, et al. KCNH2-K897T is a genetic modifier of latent congenital long-QT syndrome. Circulation. 2005; 112(9):1251–1258. doi:10.1161/CIRCULATIONAHA.105.549071. PMID: 16116052. [PubMed: 16116052]

Dumaine R, Wang Q, Keating MT, Hartmann HA, Schwartz PJ, Brown AM, Kirsch GE. Multiple mechanisms of Na+ channel-linked long-QT syndrome. Circ. Res. 1996; 78(5):916–924. PMID: 8620612. [PubMed: 8620612]

Fahmi AI, Patel M, Stevens EB, Fowden AL, John JE III, Lee K, et al. The sodium channel beta-subunit SCN3b modulates the kinetics of SCN5a and is expressed heterogeneously in sheep heart. J. Physiol. 2001; 537(3):693–700. doi:10.1113/jphysiol. 2001.012691. PMID:11744748. [PubMed: 11744748]

Fredj S, Sampson KJ, Liu H, Kass RS. Molecular basis of ranolazine block of LQT-3 mutant sodium channels: evidence for site of action. Br. J. Pharmacol. 2006; 148(1):16–24. doi:10.1038/sj.bjp. 0706709. PMID:16520744. [PubMed: 16520744]

Grant AO, Carboni MP, Neplioueva V, Starmer CF, Memmi M, Napolitano C, Priori S. Long QT syndrome, Brugada syndrome, and conduction system disease are linked to a single sodium channel mutation. J. Clin. Invest. 2002; 110(8):1201–1209. PMID:12393856. [PubMed: 12393856]

Herfst LJ, Potet F, Bezzina CR, Groenewegen WA, Le Marec M, Hoorntje TM, et al. Na^+ channel mutation leading to loss of function and non-progressive cardiac conduction defects. J. Mol. Cell. Cardiol. 2003; 35(5):549–557. doi:10.1016/S0022-2828(03) 00078-6. PMID:12738236. [PubMed: 12738236]

Huang H, Millat G, Rodriguez-Lafrasse C, Rousson R, Kugener B, Chevalier P, Chahine M. Biophysical characterization of a new SCN5A mutation S1333Y in a SIDS infant linked to long QT syndrome. FEBS Lett. 2009; 583(5):890–896. doi:10.1016/j. febslet.2009.02.007. PMID: 19302788. [PubMed: 19302788]

Jeck CD, Boyden PA. Age-related appearance of outward currents may contribute to developmental differences in ventricular repolarization. Circ. Res. 1992; 71(6):1390–1403. PMID: 1423935. [PubMed: 1423935]

Kellenberger S, West JW, Catterall WA, Scheuer T. Molecular analysis of potential hinge residues in the inactivation gate of brain type IIA Na^+ channels. J. Gen. Physiol. 1997; 109(5):607–617. doi: 10.1085/jgp.109.5.607. PMID:9154907. [PubMed: 9154907]

Kyndt F, Probst V, Potet F, Demolombe S, Chevallier JC, Baro I, et al. Novel SCN5A mutation leading either to isolated cardiac conduction defect or Brugada syndrome in a large French family. Circulation. 2001; 104(25):3081–3086. doi:10.1161/ hc5001.100834. PMID:11748104. [PubMed: 11748104]

Lehtonen A, Fodstad H, Laitinen-Forsblom P, Toivonen L, Kontula K, Swan H. Further evidence of inherited long QT syndrome gene mutations in antiarrhythmic drug-associated torsades de pointes. Heart Rhythm. 2007; 4(5):603–607. doi:10.1016/j.hrthm.2007.01.019. PMID:17467628. [PubMed: 17467628]

Li Q, Huang H, Liu G, Lam K, Rutberg J, Green MS, et al. Gain-of-function mutation of Nav1.5 in atrial fibrillation enhances cellular excitability and lowers the threshold for action potential firing. Biochem. Biophys. Res. Commun. 2009; 380(1):132–137. doi:10.1016/j.bbrc.2009.01.052. PMID: 19167345. [PubMed: 19167345]

Lupoglazoff JM, Cheav T, Baroudi G, Berthet M, Denjoy I, Cauchemez B, et al. Homozygous SCN5A mutation in long-QT syndrome with functional two-to-one atrioventricular block. Circ. Res. 2001; 89(2):E16–E21. doi:10.1161/hh1401.095087. PMID:11463728. [PubMed: 11463728]

Magyar J, Kiper CE, Dumaine R, Burgess DE, Banyasz T, Satin J. Divergent action potential morphologies reveal nonequilibrium properties of human cardiac Na channels. Cardiovasc. Res. 2004; 64(3):477–487. doi:10.1016/j.cardiores.2004. 07.014. PMID:15537501. [PubMed: 15537501]

Makita N, Bennett PB, George AL Jr. Molecular determinants of b1 subunit-induced gating modulation in voltage-dependent Na^+ channels. J. Neurosci. 1996; 16(22):7117–7127. PMID: 8929421. [PubMed: 8929421]

Makiyama T, Akao M, Shizuta S, Doi T, Nishiyama K, Oka Y, et al. A novel SCN5A gain-of-function mutation M1875T associated with familial atrial fibrillation. J. Am. Coll. Cardiol. 2008; 52(16): 1326–1334. doi:10.1016/j.jacc.2008.07.013. PMID:18929244. [PubMed: 18929244]

Maltsev VA, Sabbah HN, Higgins RS, Silverman N, Lesch M, Undrovinas AI. Novel, ultraslow inactivating sodium current in human ventricular cardiomyocytes. Circulation. 1998; 98(23):2545–2552. PMID:9843461. [PubMed: 9843461]

McCormick KA, Srinivasan J, White K, Scheuer T, Catterall WA. The extracellular domain of the b1 subunit is both necessary and sufficient for b1-like modulation of sodium channel gating. J. Biol. Chem. 1999; 274(46):32638–32646. doi:10. 1074/jbc.274.46.32638. PMID:10551818. [PubMed: 10551818]

McPhee JC, Ragsdale DS, Scheuer T, Catterall WA. A critical role for transmembrane segment IVS6 of the sodium channel alpha subunit in fast inactivation. J. Biol. Chem. 1995; 270(20):12025–12034. doi:10.1074/jbc.270.20.12025. PMID:7744852. [PubMed: 7744852]

McPhee JC, Ragsdale DS, Scheuer T, Catterall WA. A critical role for the S4-S5 intracellular loop in domain IV of the sodium channel alpha-subunit in fast inactivation. J. Biol. Chem. 1998; 273(2): 1121–1129. doi:10.1074/jbc.273.2.1121. PMID:9422778. [PubMed: 9422778]

Meadows LS, and Isom, L. Sodium channels as macromolecular complexes: implications for inherited arrhythmia syndromes. Cardiovasc. Res. 2005; 67(3):448–458. doi:10.1016/j. cardiores. 2005.04.003. PMID:15919069. [PubMed: 15919069]

Moss AJ, Zareba W, Schwarz KQ, Rosero S, McNitt S, Robinson JL. Ranolazine shortens repolarization in patients with sustained inward sodium current due to type-3 long-QT syndrome. J. Cardiovasc. Electrophysiol. 2008; 19(12):1289–1293. doi:10.1111/j.1540-8167.2008.01246.x. PMID:18662191. [PubMed: 18662191]

Nof E, Cordeiro JM, Perez GJ, Scornik FS, Calloe K, Love B, et al. A common single nucleotide polymorphism can exacerbate long-QT type 2 syndrome leading to sudden infant death. Circ. Cardiovasc. Genet. 2010; 3(2):199–206. doi:10.1161/ CIRCGENETICS.109.898569. PMID: 20181576. [PubMed: 20181576]

Plotnikov AN, Sosunov EA, Patberg KW, Anyukhovsky EP, Gainullin RZ, Shlapakova IN, et al. Cardiac memory evolves with age in association with development of the transient outward current. Circulation. 2004; 110(5):489–495. doi:10.1161/01. CIR.0000137823.64947.52. PMID: 15262840. [PubMed: 15262840]

Priori SG, Napolitano C, Giordano U, Collisani G, Memmi M. Brugada syndrome and sudden cardiac death in children. Lancet. 2000; 355(9206):808–809. doi:10.1016/S0140-6736(99)05277-0. PMID: 10711933. [PubMed: 10711933]

Qu Y, Isom LL, Westenbroek RE, Rogers JC, Tanada TN, McCormick KA, et al. Modulation of cardiac Na^+ channel expression in Xenopus oocytes by b1 subunits. J. Biol. Chem. 1995; 270(43): 25696–25701. doi:10.1074/jbc.270.43.25696. PMID:7592748. [PubMed: 7592748]

Remme CA, Bezzina CR. Genetic modulation of cardiac repolarization reserve. Heart Rhythm. 2007; 4(5):608–610. doi:10.1016/j.hrthm.2007.02.025. PMID:17467629. [PubMed: 17467629]

Remme CA, Wilde AA, Bezzina CR. Cardiac sodium channel overlap syndromes: different faces of SCN5A mutations. Trends Cardiovasc. Med. 2008; 18(3):78–87. doi:10.1016/j.tcm.2008. 01.002. PMID:18436145. [PubMed: 18436145]

Ruan Y, Denegri M, Liu N, Bachetti T, Seregni M, Morotti S, et al. Trafficking defects and gating abnormalities of a novel SCN5A mutation question gene-specific therapy in long QT syndrome type 3. Circ. Res. 2010; 106(8):1374–1383. doi:10.1161/ CIRCRESAHA.110.218891. PMID: 20339117. [PubMed: 20339117]

Schwartz PJ, Garson A Jr, Paul T, Stramba-Badiale M, Vetter VL, Wren C. European Society of Cardiology. 2002. Guidelines for the interpretation of the neonatal electrocardiogram. A task force of the European Society of Cardiology. Eur. Heart J. 23(17):1329–1344. doi:10.1053/euhj. 2002.3274. PMID: 12269267. [PubMed: 12269267]

Shimoni Y, Fiset C, Clark RB, Dixon JE, McKinnon D, Giles WR. Thyroid hormone regulates postnatal expression of transient K^+ channel isoforms in rat ventricle. J. Physiol. 1997; 500(1):65–73. PMID:9097933. [PubMed: 9097933]

Smith MR, Goldin AL. Interaction between the sodium channel inactivation linker and domain III S4-S5. Biophys. J. 1997; 73(4):1885–1895. doi:10.1016/S0006-3495(97)78219-5. PMID: 9336184. [PubMed: 9336184]

Song Y, Shryock JC, Wu L, Belardinelli L. Antagonism by ranolazine of the pro-arrhythmic effects of increasing late INa in guinea pig ventricular myocytes. J. Cardiovasc. Pharmacol. 2004; 44(2): 192–199. doi:10.1097/00005344-200408000-00008. PMID:15243300. [PubMed: 15243300]

Spitzer KW, Pollard AE, Yang L, Zaniboni M, Cordeiro JM, Huelsing DJ. Cell-to-cell electrical interactions during early and late repolarization. J. Cardiovasc. Electrophysiol. 2006; 17(s1 Suppl. 1):S8–S14. doi:10.1111/j.1540-8167.2006.00379.x. PMID:16686687. [PubMed: 16686687]

Trépanier-Boulay V, Lupien M-A, St-Michel C, Fiset C. Postnatal development of atrial repolarization in the mouse. Cardiovasc. Res. 2004; 64(1):84–93. doi:10.1016/j.cardiores.2004.06. 002. PMID: 15364616. [PubMed: 15364616]

Valdivia CR, Ackerman MJ, Tester DJ, Wada T, McCormack J, Ye B, Makielski JC. A novel SCN5A arrhythmia mutation, M1766L, with expression defect rescued by mexiletine. Cardiovasc. Res. 2002; 55(2):279–289. doi:10.1016/S0008-6363(02) 00445-5. PMID:12123767. [PubMed: 12123767]

Veldkamp MW, Viswanathan PC, Bezzina C, Baartscheer A, Wilde AA, Balser JR. Two distinct congenital arrhythmias evoked by a multidysfunctional Na(+) channel. Circ. Res. 2000; 86(9):E91–E97. PMID:10807877. [PubMed: 10807877]

Wang DW, Desai RR, Crotti L, Arnestad M, Insolia R, Pedrazzini M, et al. Cardiac sodium channel dysfunction in sudden infant death syndrome. Circulation. 2007; 115(3):368–376. doi:10.1161/CIRCULATIONAHA.106.646513. PMID:17210841. [PubMed: 17210841]

Wang DW, Crotti L, Shimizu W, Pedrazzini M, Cantu F, De Filippo P, et al. Malignant perinatal variant of long-QT syndrome caused by a profoundly dysfunctional cardiac sodiumchannel. Circ. Arrhythm. Electrophysiol. 2008; 1(5):370–378. doi:10. 1161/CIRCEP.108.788349. PMID: 19808432. [PubMed: 19808432]

Wedekind H, Smits JP, Schulze-Bahr E, Arnold R, Veldkamp MW, Bajanowski T, et al. De novo mutation in the SCN5A gene associated with early onset of sudden infant death. Circulation. 2001; 104(10):1158–1164. doi:10.1161/hc3501.095361. PMID:11535573. [PubMed: 11535573]

Wegener FT, Ehrlich JR, Hohnloser SH. Amiodarone-associated macroscopic T-wave alternans and torsade de pointes unmasking the inherited long QT syndrome. Europace. 2008; 10(1):112–113. doi:10.1093/europace/eum252. PMID:18006559. [PubMed: 18006559]

West JW, Patton DE, Scheuer T, Wang Y, Goldin AL, Catterall WA. A cluster of hydrophobic amino acid residues required for fast Na(+)-channel inactivation. Proc. Natl. Acad. Sci. U.S.A. 1992; 89(22):10910–10914. doi:10.1073/pnas.89.22. 10910. PMID:1332060. [PubMed: 1332060]

Wu L, Shryock JC, Song Y, Li Y, Antzelevitch C, Belardinelli L. Antiarrhythmic effects of ranolazine in a guinea pig in vitro model of long-QT syndrome. J. Pharmacol. Exp. Ther. 2004; 310(2):599–605. doi:10.1124/jpet.104.066100. PMID: 15031300. [PubMed: 15031300]

Wu L, Rajamani S, Shryock JC, Li H, Ruskin J, Antzelevitch C, Belardinelli L. Augmentation of late sodium current unmasks the proarrhythmic effects of amiodarone. Cardiovasc. Res. 2008; 77(3): 481–488. doi:10.1093/cvr/cvm069. PMID:18006430. [PubMed: 18006430]

Zimmer T, Surber R. SCN5A channelopathies-an update on mutations and mechanisms. Prog. Biophys. Mol. Biol. 2008; 98(2-3):120–136. doi:10.1016/j.pbiomolbio.2008.10.005. PMID: 19027780. [PubMed: 19027780]

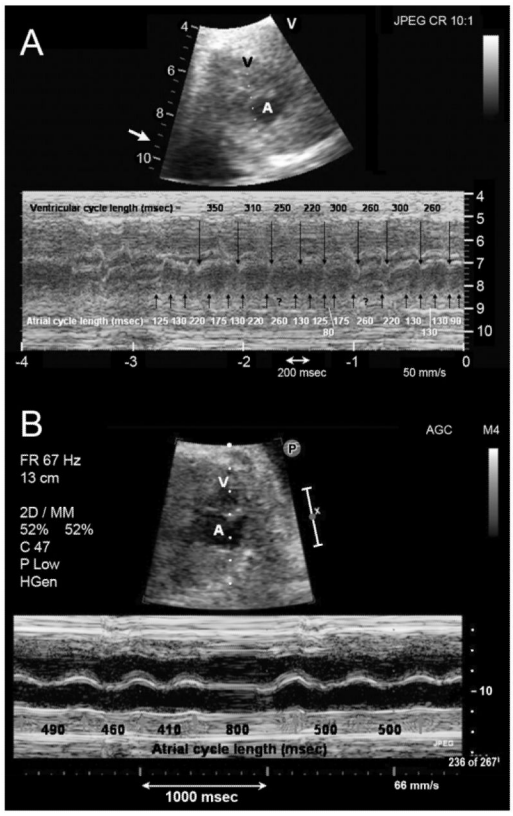

Fig. 1.

(A) Two-dimensional fetal echocardiogram at 29 weeks gestation showing a frame from sector scan (above) and accompanying m-mode (below). Illustrated are mechanical atrial events at a very rapid and irregular rate (indicated by upward pointing arrows) and slower mechanical ventricular events (indicated by downward pointing arrows). (B) Fetal echocardiogram using the same format and obtained 3 days later after administration of sotalol to the mother, illustrating a normal atrial rate (indicated by upward pointing arrows) and a sinus pause. A, atrium; V, ventricle.

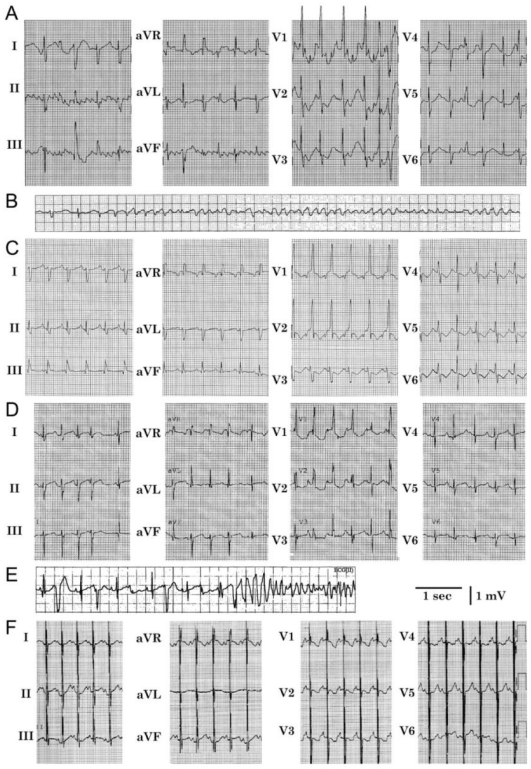

Fig. 2.

(A) Twelve lead ECG of the proband soon after birth showing atrial flutter. (B) This deteriorated into ventricular fibrillation, requiring defibrillation. (C) Sinus rhythm on the 5th day of life, demonstrating intraventricular conduction delay. (D) During treatment with amiodarone on the 10th day of life, there was prolongation of the QTc interval (491 ms in V5 during period of stable sinus rhythm). (E) Also on the 10th day of life, following a short–long–short QRS sequence, torsade de pointes occurred. (F) Twelve lead ECG at 23 months of age while drug-free, showing normal QRS duration and QTc interval prolongation (466 ms). Pacing spikes account for pseudofusion.

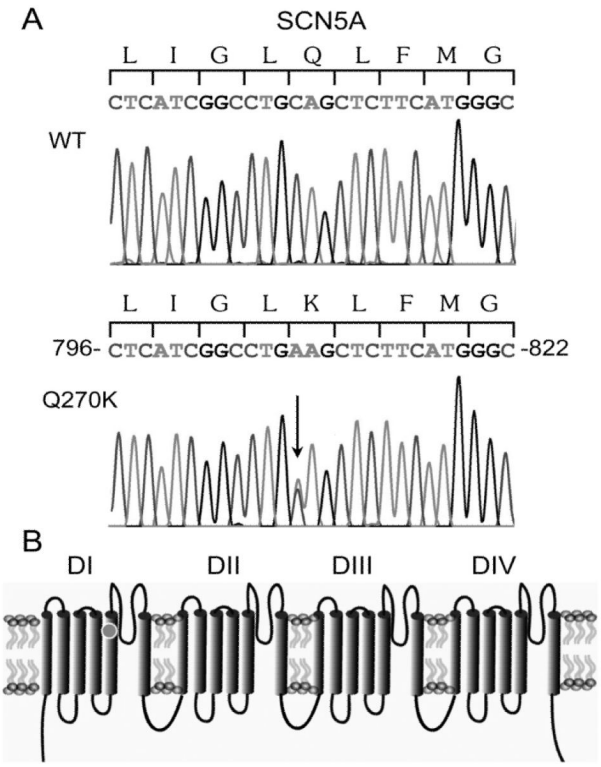

Fig. 3.

Electropherogram of the patient's DNA showing a heterozygous C to A transition at nucleotide position 808 in exon 7 in SCN5A (A), resulting in a substitution of glutamine (Q) to a lysine (K) at position 270 (Q270K) in S5 of the first domain (D1) of the $Na_v1.5$ sodium channel, marked by a dot in (B).

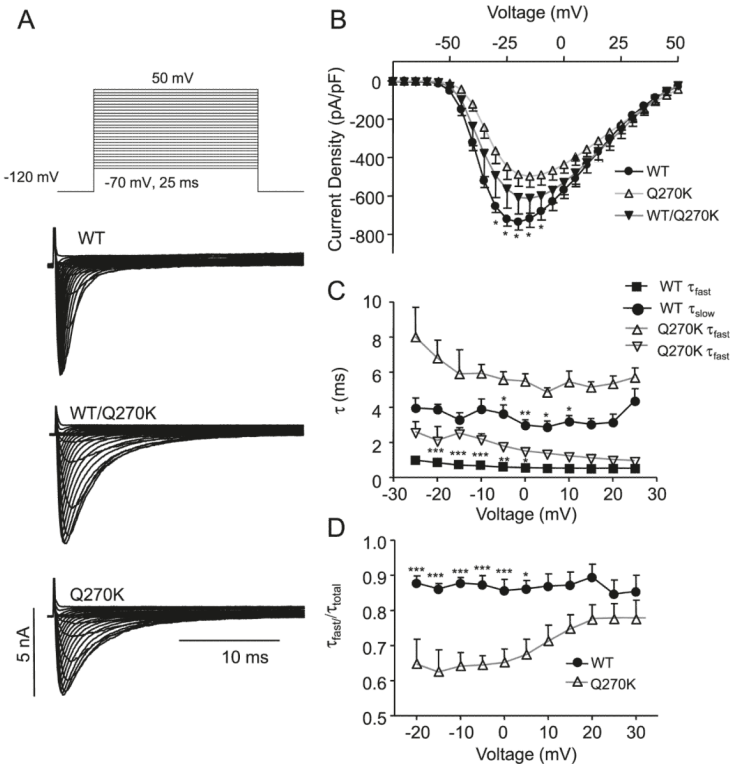

Fig. 4.

Whole-cel1 current recordings for $Na_v1.5$ wild type (WT) ($n = 8$), WT/Q270K (1:1 ratio, $n = 6$), and Q270K ($n = 8$). (A) Representative recordings. (B) Peak current density as a function of voltage. The asterisks indicate significant difference between WT and Q270K: *, $p < 0.05$; **, $p < 0.01$; and ***, $p < 0.001$. The difference between WT and WT/Q270K did not reach statistical significance. (C) Double exponential functions fit to the current decay and the resulting time-constants (τ_{slow} and τ_{fast}) plotted as a function of voltage. (D) The relative weight of the pre-exponential factors for τ_{fast}/τ_{total} as a function of voltage.

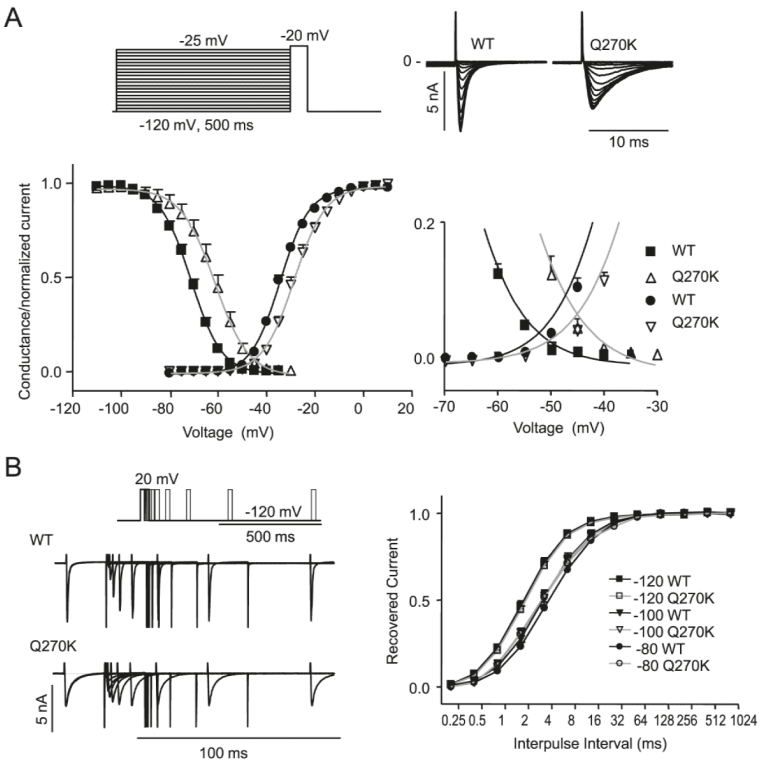

Fig. 5.

Activation and steady state-inactivation relation for $Na_v1.5$ wild type (WT) (n = 9) and Q270K (n = 6). (A) Activation curves were calculated by normalizing the currents shown in Fig. 4 to (V_m–E_K). Steady-state inactivation was determined using the protocol shown in the inset. Peak currents at −20 mV were normalized and plotted against the conditioning potential, and Boltzmann equations were fit to the data points. The overlap regions of the 2 relationships are enlarged. (B) Time-dependent recovery from inactivation for WT and Q270K. Currents were activated by a 2-pulse protocol from a holding of either −120 mV, −100 mV, or −80 mV. The fraction of recovered current was plotted as a function of interpulse interval, and single exponential functions were fitted to the data.

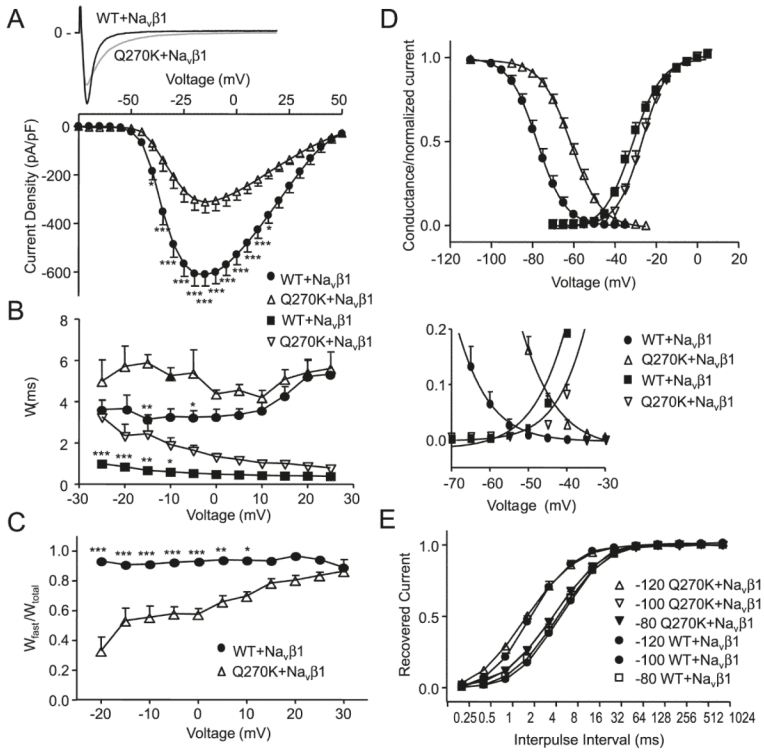

Fig. 6.

Whole-cell current recordings for $Na_v1.5$ wild type (WT) (n = 11) and Q270K (n = 10) co-expressed with $Na_v\beta1$ (1:1 ratio). (A) Representative currents and peak current densities shown as a function of voltage. (B) Double exponential functions were fit to current decay and the time-constants (τ_{slow} and τ_{fast}) are shown as a function of voltage. (C) Relative weight of the pre-exponential factors. (D) Activation curves were calculated by normalizing the currents shown in A to (V_m–E_K). Steady-state inactivation was measured and peak currents at −20 mV were normalized, plotted against the conditioning potential, and Boltzmann equations were fit to the data points. The overlap regions are enlarged. (E) Time-dependent recovery from inactivation for WT/ $Na_v\beta1$ and Q270K/$Na_v\beta1$. Currents were activated by a 2-pulse protocol from a holding of either −120 mV, −100 mV, or −80 mV. The fraction of recovered current was plotted as a function of interpulse interval and single exponential functions were fit to the data. *, $p < 0.05$; **, $p < 0.01$; and ***, $p < 0.001$.

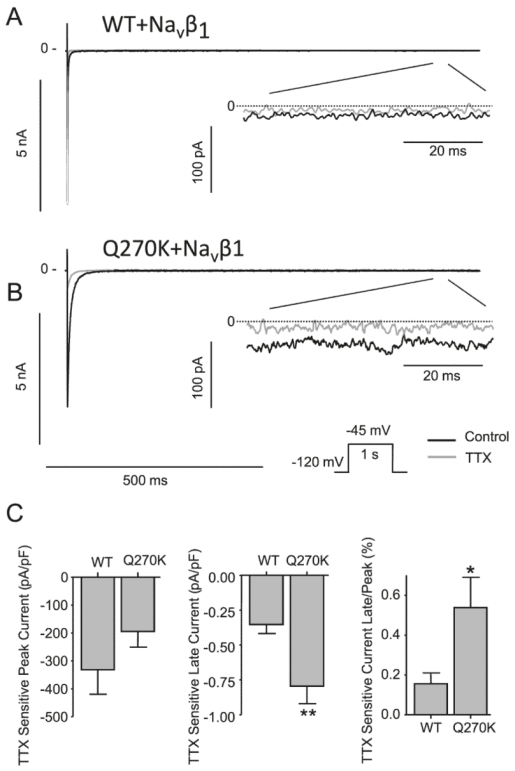

Fig. 7.

Effect of 10 μmol/L tetrodotoxin (TTX) on $Na_v1.5$ wild type (WT) (n = 5) and Q270K (n = 5) co-expressed with $Na_v\beta1$ (1:1 ratio). Currents were activated by a 1 s step to −45 mV from a holding potential of −120 mV at a frequency of 0.25 Hz. (A) Representative WT recordings in absence or presence of TTX. For comparison, the peak and late current are shown at different scales. (B) Representative Q270K recordings. (C) Summarized data of the effect of TTX on current density. Currents in presence of TTX were digitally subtracted from currents recorded in the absence of TTX to determine the TTX-sensitive current. Late current was measured as mean current after 950–990 ms and the ratio between the TTX-sensitive peak and late current was calculated for WT and Q270K. *, $p < 0.05$ and **, $p < 0.01$.

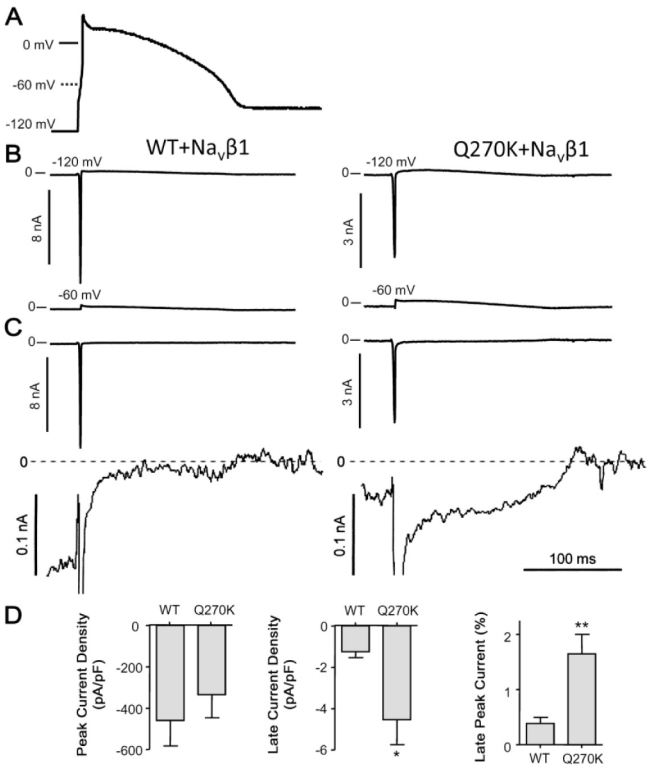

Fig. 8.

Wild type (WT) (n = 7) and Q270K (n = 6) co-expressed with Na$_v$β1 (1:1 ratio). An action potential previously recorded from an isolated neonate canine ventricular cardiomyocyte paced at 1 Hz was used as command (A). (B) The command action potential was modified so that either a holding potential of −120 mV or −60 mV was imposed. (C) The recordings obtained using −60 mV as holding was digitally subtracted from the recordings obtained at −120 mV. For comparison, the peak and late current are shown at different scales. (D) Summary data of peak and late WT/Na$_v$β1 and Q270K/Na$_v$β1 current, as well as the ratio between late and peak current. Late current was measured as mean current 50 to 55 ms after the peak, corresponding to a potential of 22–23 mV. *, $p < 0.05$ and **, $p < 0.01$.

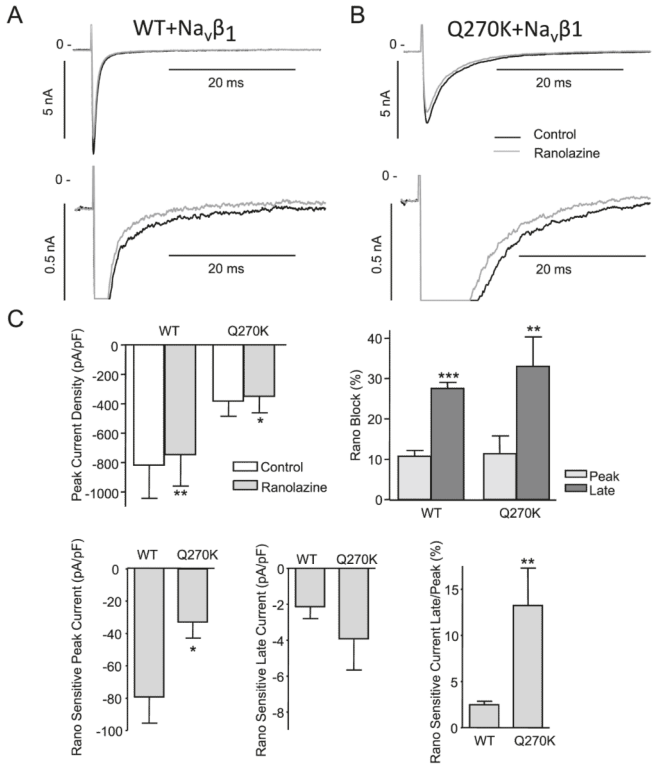

Fig. 9.

Effect of 50 μmol/L ranolazine on wild type (WT) (n = 7) and Q270K (n = 4) co-expressed with Na$_v$β1 (1:1 ratio). Currents were activated by −20 mV step from a holding potential of −120 mV at a frequency of 0.25 Hz. (A) Representative WT recordings in the absence or presence of ranolazine. For comparison, the peak and late current are shown at different scales. (B) Representative Q270K recordings. (C) Summarized data of the effect of ranolazine on peak current density and percentage block of peak and late currents. The ranolazine sensitive currents were determined by digitally subtracting currents in presence of ranolazine from control. The late currents were determined as mean currents 45 to 50 ms after the peak and the ratio between the ranolazine sensitive peak and late current was calculated for WT and Q270K. *, $p < 0.05$; **, $p < 0.01$; and ***, $p < 0.001$.